sciendo

Strojnícky časopis – *Journal of* MECHANICAL ENGINEERING,
VOL 72 (2022), NO 1, 77 – 88

STU SjF

INFLUENCE OF THE SELECTED SIEVING PARAMETERS ON THE SIEVING EFFICIENCY OF MATERIAL MCC AVICEL PH102

JEZSÓ Kristian[1], PECIAR Peter[1]

[1]*Slovak University of Technology in Bratislava, Faculty of Mechanical Engineering, Institute of Process Engineering, Námestie Slobody 17, 812 31 Bratislava, Slovakia*
**e-mail: kristian.jezso@stuba.sk, peter.peciar@stuba.sk*

Abstract: Sieving or screening plays a crucial role in the processing of particulate materials. The sieving process is affected by many factors, including the selection of suitable sieving equipment. Several experiments were carried out to examine the influence of three basic sieving parameters on process efficiency. The investigated material was MCC Avicel PH102, which is widely used as an excipient in the pharmaceutical industry. The three mentioned parameters were sample mass, sieving duration, and vibration amplitude. It was necessary to find a suitable method to evaluate screening efficiency.

KEYWORDS: particulate material, MCC Avicel PH102, sieving, sieving equipment, efficiency

1 Introduction

Sieving and screening machines are among the most widely used devices in the production and processing of particulate material [2], and are mainly used in the pharmaceutical, food, chemical, and mining industry. The equipment used in these areas must meet ever-increasing demands for accuracy and performance. For this reason, it is important to maximize screening efficiency [9].

The term ‘sieving’ is used to refer to a batch sizing process, as distinct from screening, which usually means a continuous process [1]. The particle size distribution of product fractions can have a significant influence on the properties of the material, for instance on bulk density or on specific surface area. The authors found in an article [24] that the particle size distribution of flour affects baking quality, since the content of proteins and minerals varies with the size of the particles. The dependence of protein content on particle size was also confirmed in [1]. The size of rice flour particles also affects the texture and hardness of the product [23]. Furthermore, in [8] it was confirmed that as particle size decreases, the moisture content of the coal increases significantly. These examples show that increasing sieving efficiency has a significant impact on quality.

In fact, the screening and sieving process, influenced by many factors, is governed by the laws of physics and fluid mechanics, which makes it a complex task. Factors affecting the movement of individual particles and thus the efficiency of the process can be divided into three groups [21]. The effects of these parameters have been investigated by many authors. The first group includes the properties of the raw material, such as particle size distribution [12, 15], particle shape [5, 11, 20], moisture content [1, 8]. Factors that depend on the design of the equipment used belong to a second group, and includes the shape and size of the screen openings [5, 8, 11, 12, 20, 26, 27], type and material [5, 8], screen inclination angle [2, 4, 6, 11, 14, 21, 26, 27], vibration mode (linear, circular, elliptical) [2, 7], direction [4, 6, 14, 19, 22], vibration amplitude [2, 11, 14, 19, 21, 27] and frequency [2, 4, 6, 11, 14, 19, 22, 27]. The third

DOI: 10.2478/scjme-2022-0008, Print ISSN 0039-2472, On-line ISSN 2450-5471

group includes factors that characterise the sieving/screening process itself, such as mass flow (in the case of a continuous process) or the amount of material fed in (in the case of a batch process) [5, 8, 11, 12, 20, 22], sieving duration [1, 3, 16] and the influence of particle layer thickness [8, 10, 11, 15]. The sieving/screening process is also accompanied by blinding of the screen apertures, which is mainly caused by near mesh-sized particles. This phenomenon results a reduction of the effective screening area, and was analysed by the authors in studies [3, 16]. The aim is to optimise the whole process to maximise efficiency as much as possible, but it is important to keep in mind that increasing the amount of material fed adversely affects mesh wear. Wear problems were examined in articles [4, 6, 14]. The effects of the above-mentioned factors on particle motion and efficiency are often investigated by use of the discrete element method (DEM) [2, 4-8, 11-14, 19, 20, 22, 26].

2. Sieving efficiency

The efficiency of the sieving process can be derived by the use of a simple mass balance [30, 31]. The sieving efficiency defines the ratio to which the real process approaches the ideal process. Usually, the efficiency is related to the sieving surface and consists of two recoveries. The first recovery characterizes the oversize fraction – r_A, the second recovery, the undersize fraction – r_B. The mass balance shows that the recovery of particles that have a diameter larger than aperture size D_a can be expressed as follows:

$$r_A = \frac{A\ R_A}{F\ R_F} = \frac{R_A(R_F - R_B)}{R_F(R_A - R_B)} \tag{1}$$

and the recovery of particles which have a diameter equal to or smaller than the aperture size D_a can be written as the following equation:

$$r_B = \frac{B\ (1 - R_B)}{F\ (1 - R_F)} = \frac{(1 - R_B)(R_A - R_F)}{(1 - R_F)(R_A - R_B)} \tag{2}$$

where A is the mass of the oversized product, B is the mass of the undersized product, F is the mass of the raw material, R_A is the mass fraction of particles which have a diameter larger than aperture size D_a in the oversized product, R_B is the mass fraction of particles which have a diameter larger than aperture size D_a in the undersized product, R_F is the mass fraction of particles which have a diameter larger than the aperture size in the raw material, r_A is the recovery of coarse product and r_B is the recovery of fine product.

The total classification efficiency η can be calculated in two ways, either by multiplying individual recoveries as in [25, 31], in which case the total classification efficiency can be expressed as follows:

$$\eta = r_A r_B 100 \tag{3}$$

or by summing up these recoveries [21, 27, 30], then the total classification efficiency can be written as:

$$\eta = (r_A + r_B - 1)100 \tag{4}$$

A different form of calculation was chosen by the authors in papers [8, 10, 14], where they expressed the mass fractions differently, but this solution gives the same results as Eq. (3). In some cases, such as simulations with spherical particles, is used a simplified form of efficiency calculations, which excludes the occurrence of particles larger than D_a in the undersized product.

Eq. (3) and (4) are very convenient for use in the case of a single-sieve surface. Here the raw material is divided into 2 fractions, oversized product and undersized product. By analysing

these fractions, the parameters to Eq. (1) and (2) can be determined. However, this is no longer clear in the case of measurements with multiple sieving surfaces because it is questionable whether, in the case of a specific sieve only the oversize product and undersize product directly above or below the sieve should be taken into account, or whether other fractions should also be included in the calculation. It is not the same whether, in the case of a sieve with a 200 µm aperture size, only the fraction on the sieve with a 100 µm aperture size is considered as undersize fraction or also the other fractions below. For this reason, in this paper the evaluation of sieving efficiency was performed in a slightly different way. Efficiency was defined as the ratio of the mass of particles belonging to a given fraction on a given sieve to the mass of particles that should theoretically be in that fraction at the end of the process. Put simply: what percentage of the mass at the end of the sieving process was in the right place in the right fraction. The equations shown above will always assign the efficiency to a given sieve, while the efficiency used in this paper expresses how efficiently particles of a given fraction get to the desired sieve and how efficiently they stay there.

3 Experimental material

Microcrystalline cellulose (MCC) is one of the most widely used pharmaceutical excipients for the uniaxial pressing of tablets [17, 32]. In the experiments described in this paper, samples of MCC Avicel PH102 from FMC BioPolymer were used. The particle size distribution of the experimental material was measured using the Malvern Mastersizer 3000 laser analyser with a dry dispersion unit. MS3000 uses the volume of the particle to measure its size through the volume equivalent diameter [18]. The output of such an analysis is shown in Fig. 1a). It can be seen that Avicel PH102 is a polydisperse material in which particles as small as a few micrometers to particles over 300 µm are present. Fig. 1b) shows an electron microscopy image of Avicel PH102. It should be noted that the present particles of the raw material have a non-spherical angular shape, which causes deviations in the results.

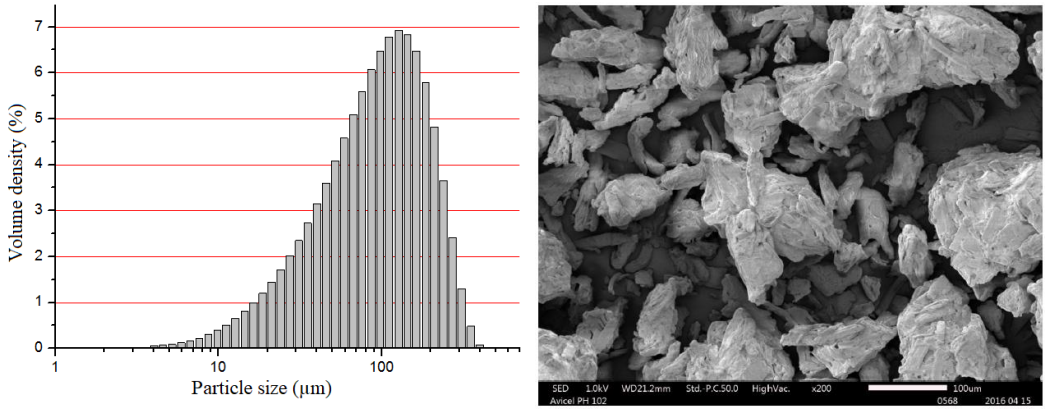

a) *b)*

Fig.1. Avicel PH102: a) particle size distribution; b) electron microscopy image [32]

4 Experimental measurements

4.1 Sieving

For sieve analysis, Retsch AS 200 sieving equipment, with adjustable parameters was used: vibration amplitude (max 3 mm = 100 %) and sieving duration (from 1 min to 99 min). Based on the particle size distribution curve (Fig. 1a), sieves with aperture sizes of 63 µm, 100 µm, 200 µm and 315 µm were selected.

4.2 Measurement process

During the initial measurements, it was found that the minimum amplitude that has any demonstrable effect on particle motion is 40 %. This value was chosen as an initial value, others were chosen in increments of 20 %, so that the amplitudes at which the experiments were carried out were 40 %, 60 %, 80 %, and 100 %. The second varying parameter was sieving duration (1 min, 3 min, 6 min, and 9 min). The masses of the input raw material were 25 g, 50 g, and 75 g. A small sample amount was taken from each fraction for laser analysis by an MS 3000 analyser. Each measurement was performed 3 times, with the average taken as a result.

4.3 Measurement evaluation methodology

During an efficiency calculation, 2 cases are always compared: real and ideal. An ideal sieve sharply separates the feed into 2 fractions. Such an ideal process would define the cut diameter, which is the aperture size of the sieve. The results of the analysis of the raw material particle size distribution are shown in Table 1, where the sieve aperture sizes (63 µm, 100 µm, 200 µm, and 315 µm) are also indicated. Using these data, it is possible to calculate the amount of material that should be present on each sieve at the end of the process. When 4 sieves are used, there are a maximum 5 fractions at the end of the sieving. The fraction which is found at the end of the process at the bottom of the set of sieves, i.e. in the pan, is referred to as fraction 0. The next fraction, located at the end of the classification on the 63 µm sieve, is referred to as fraction 63, and so on. Based on Table 1, at the end of the ideal process in fraction 0 (i.e. below the sieve with 63 µm aperture size, in the pan), 31,22 % of the feed material should be present. 23,23 % of the input material should be in fraction 63, 32,8 % in fraction 100, 12,18 % in fraction 200, and 0,55 % in fraction 315.

Table 1. Particle size distribution of Avicel PH102

Particle size (µm)	Volume density (%)	Particle size (µm)	Volume density (%)	Particle size (µm)	Volume density (%)	Particle size (µm)	Volume density (%)
3,12	0	11,2	0,51	40,1	3,15	144	6,84
3,55	0	12,7	0,65	45,6	3,6	163	6,47
4,03	0,06	14,5	0,81	51,8	4,08	186	5,79
4,58	0,07	16,4	0,99	58,9	4,58	211	4,82
5,21	0,09	18,7	1,2	66,9	5,09	240	3,65
5,92	0,12	21,2	1,44	76	5,59	272	2,41
6,72	0,16	24,1	1,71	86,4	6,07	310	1,3
7,64	0,22	27,4	2,01	98,1	6,48	352	0,48
8,68	0,3	31,1	2,35	111	6,78	400	0,07
9,86	0,39	35,3	2,73	127	6,92	454	0

200 63 315 100

The efficiency calculation will be explained with a concrete example. The results of the sieve analysis are shown in Table 2. The sieving parameters were as follows: amplitude – 100 %, sieving duration – 1 min.

Table 2. Sieve analysis data of the selected test

Fraction number (-)	Mass of fractions (g)	Raw material mass (g)
0	7,55	
63	6,07	
100	9,44	
200	1,63	
315	0,03	
Σ	24,72	25,57

It can be seen that the input mass of the raw material and the sum of the masses of the individual fractions are not the same. This represents sieving loss, which results mainly from sieve blinding and the attachment of fine particles to the sieve surface. These losses were within 5 %, which corresponds to the loss values reported in [1].

Different types of Avicel have been investigated in articles [28, 29, 32, 34]. The results show that the particle density is not a function of the particle size. In such cases, according to [33], the volume distribution of the particulate material is the same as the mass distribution. Table 2 shows that in this test the mass of the raw material was 25,57 g. Using Table 1, the masses of the individual fractions can be calculated as they would ideally be. These data are shown in Table 3.

Table 3. Masses of the fractions in the case of selected test – ideal case

Raw material mass (g)	Mass of particles in the feed (g) (0 - 63 µm)	Mass of particles in the feed (g) (63 - 100 µm)	Mass of particles in the feed (g) (100 - 200 µm)	Mass of particles in the feed (g) (200 - 315 µm)	Mass of particles in the feed (g) (over 315 µm)
25,57	7,98	5,94	8,39	3,11	0,14

After the sieve analysis was performed, the fractions on the sieves were analysed. In the case of the selected test, only 4 fractions were analysed because the mass of the fraction on the sieve with 315 µm aperture size (0,03 g) was insufficient for laser analysis. For all fractions, the result was a particle size distribution curve, just as for the raw material. Since the particle size distribution curves were available from laser analysis and the masses of the individual fractions were available from the sieve analysis, the absolute mass distribution of the particles in each fraction could be calculated by combining these two measurements. The results are shown in Table 4.

Table 4. Absolute mass of particles in each fraction

Fraction number (-)	Mass of particles in the given fraction (g) (0 - 63 µm)	Mass of particles in the given fraction (g) (63 - 100 µm)	Mass of particles in the given fraction (g) (100 - 200 µm)	Mass of particles in the given fraction (g) (200 - 315 µm)	Mass of particles in the given fraction (g) (over 315 µm)
0	5,94	1,44	0,18	0,00	0,00
63	1,53	2,85	1,66	0,03	0,00
100	0,29	1,53	5,81	1,79	0,02
200	0,04	0,00	0,38	1,04	0,17
315	insufficient amount of fraction				

Based on Table 2, fraction 0 weighed 7,55 g. After laser analysis, it was calculated that this fraction contained 5,94 g of particles with sizes from 0 µm to 63 µm, 1,44 g of particles with sizes from 63 µm to 100 µm, and 0,18 g of particles with sizes from 100 µm to 200 µm. The highlighted cells represent the material that should be present in the given fraction. Ideally, fraction 0 contains only particles up to 63 µm in size; fraction 63 contains only particles from 63 µm to 100 µm in size; etc. i.e. the material is distributed along this diagonal, only in the highlighted cells. There followed a comparison of the ideal – real states. In fraction 0, there were 5,94 g of particles that were up to 63 µm in size. However, there were 7,98 g in the raw material, so the recovery (yield) is their ratio, that is 0,744. This means that 74,4 % of the particles with sizes from 0 to 63 µm at the end of the measurement were in the fraction where these particles should ideally be, in the pan, below the sieve with 63 µm openings. This number was taken as efficiency. The same methodology was used for the other fractions too. The results of these calculations are shown in Table 5.

Table 5. Recoveries of fractions

Fraction number (-)	Recovery of particles in the given fraction (g) (0 - 63 µm)	Recovery of particles in the given fraction (g) (63 - 100 µm)	Recovery of particles in the given fraction (g) (100 - 200 µm)	Recovery of particles in the given fraction (g) (200 - 315 µm)	Recovery of particles in the given fraction (g) (over 315 µm)
0	0,744	0,242	0,021	0,000	0,000
63	0,191	0,480	0,198	0,010	0,000
100	0,036	0,257	0,693	0,576	0,156
200	0,005	0,000	0,046	0,334	1,191
315	insufficient amount of fraction				
Σ	0,976	0,979	0,958	0,920	

Ideally, value 1 would be along the diagonal, i.e. in the highlighted cells; everywhere else, 0. After summing up the individual recoveries in a vertical direction, it can be seen that they are close to 1 (100 %); everywhere the values are above 0,9. This means that for example the efficiency in the case of fraction 63 is not so low due to various "losses" (0,48 = 48 %), but because a certain amount of material (0,242 = 24,2 % and 0,257 = 25,7 %) has passed through the sieve with an aperture size of 63 µm and has not passed through the sieve with an aperture size of 100 µm, respectively. The measurement in this section is characterised by five recoveries / efficiencies, i.e. one for each fraction. In the case of selected test only by four, because the amount of fraction 315 was insufficient for the analysis. The aim was to characterize each measurement with one number, and this was done through a weighted average. This procedure was repeated for each measurement, and in this way, at the end, 48 efficiencies were available to characterize the 48 tests. These results are shown in Figures 2 to 4, each time for one constant parameter.

4.4 Results

The graphs in Figures 2 to 4 show the dependence of the sieving efficiency on the magnitude of the amplitudes, on the duration of the sieving, and on the mass of the raw material. Each point on these graphs represents a single measurement at different parameters.

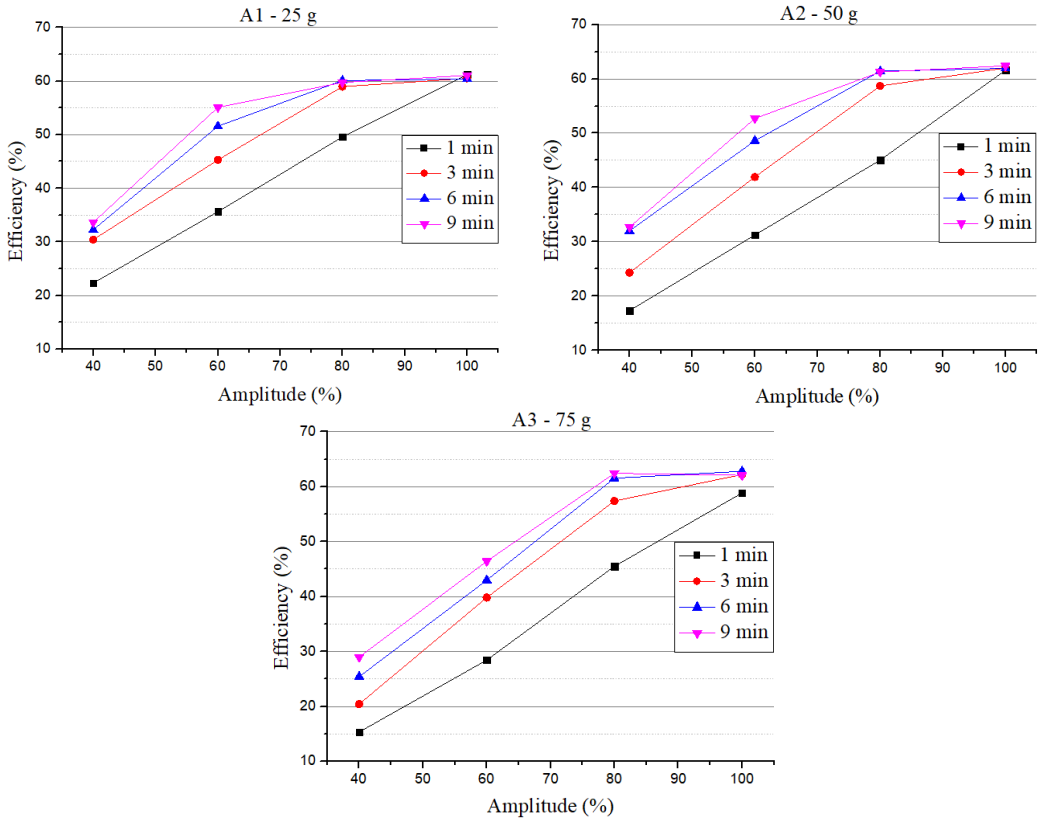

Fig. 2. Efficiency values at equal masses: A1 – 25 g; A2 – 50 g; A3 – 75 g

The results in Fig. 2 confirm the assumption that as the amplitude increases and the sieving duration increases, the efficiency of the process also increases. It can be seen that the curves that show the results at constant times grow linearly. A break occurs only when the next linear value should already be above 60 %. The maximum achievable efficiency in these experiments was slightly greater than 60 %. In industrial processes it is good and advantageous to know the parameters at which maximum efficiency has been reached, so that further increasing of the amplitude or the sieving duration will not increase the efficiency. At excessive sieving durations and amplitudes, there will be a higher number of particle collisions, with greater impact, leading to mass losses at particle level.

Fig. 3 shows the same measurement results as in the previous figure (Fig. 2), only they are constructed differently. It can be seen that the efficiency threshold, ca. 60 %, was reached at 100 % amplitude (3 mm) even with 1 min sieving duration. At lower amplitudes, the process efficiency was already influenced by the process durations. Furthermore, the amount of raw material also had a small influence on the results. This fact is particularly noticeable at lower amplitudes, since these curves show decreasing trends with increasing input material mass.

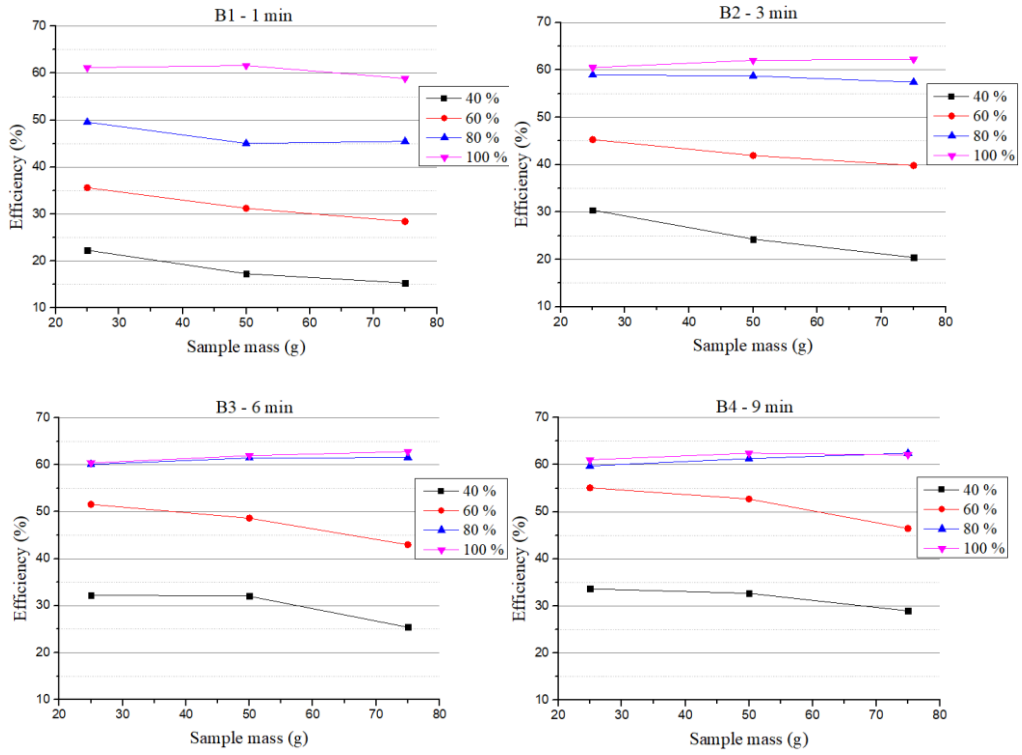

Fig. 3. Efficiency values at equal sieving durations:
B1 – 1 min; B2 – 3 min; B3 – 6 min; B4 – 9 min (curve parameters: amplitudes)

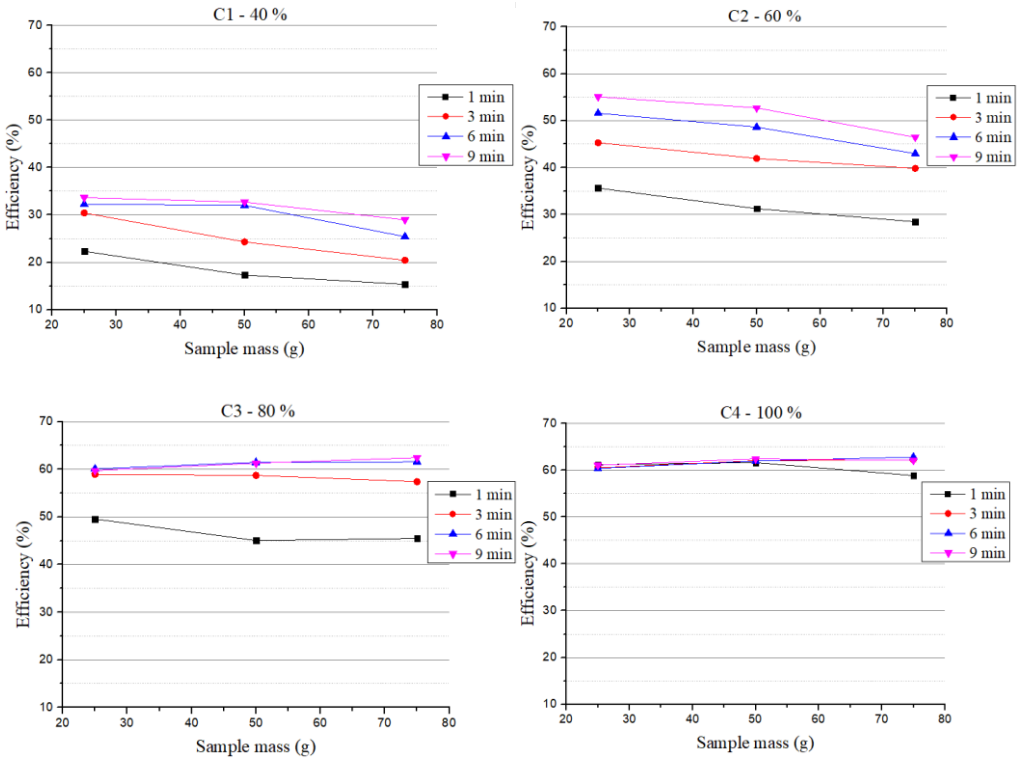

Fig. 4. Efficiency values at equal amplitudes C1 – 40 %; C2 – 60 %; C3 – 80 %; C4 – 100 %

Vibration amplitude has the most significant influence on sieving efficiency; sieving duration is only secondary. This can be seen in Fig. 4, especially at smaller amplitudes (C1 – C2). Gradually increasing the sieving duration does increase the efficiency, but this change in efficiency is not proportional to the time changes. Fig. 5 shows this dependency with 60 %

amplitude measurements. The efficiency growth is always positive with increases in the duration of the sieving, but the slope of the lines joining the two efficiencies is shallower with increasing time. This is also in agreement with the paper [1], where it is written that particle penetration is more significant at the beginning of the process, and that tendency decreases over time.

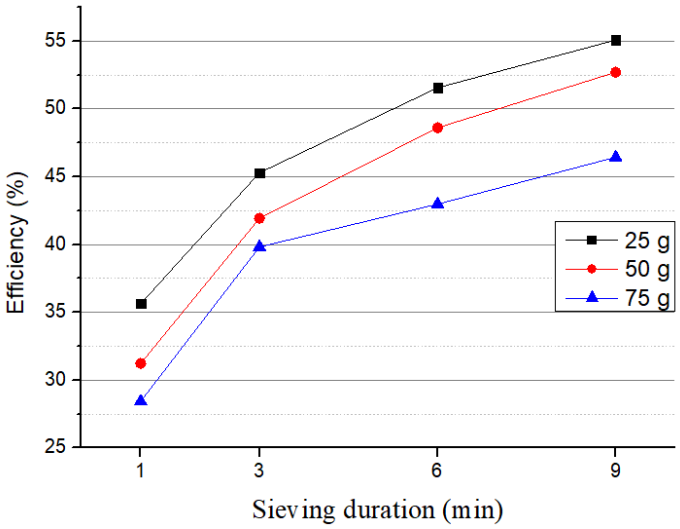

Fig. 5. Efficiency dependence on sieving duration with variable raw material masses (amplitude – 60 %)

Conclusions

During the measurements, 3 parameters were varied: the mass of the input material, the amplitude of the vibrations, and the duration of the tests. Amplitude has the greatest impact on efficiency, followed by the duration of the process, while the mass of the raw material has the least effect. With regard to mass, it should be noted that a good range has been chosen. This means that for small input material volumes, the blinding of the apertures does not play such a large role. In cases of larger volumes or continuous process, blinding can already significantly reduce the effective sieve area.

Characterising a three-dimensional particle with one dimension can only be done with sufficient accuracy for spherical particles. In any other case, it is more or less an idealization. This was the case in this study, because Avicel particles differ from this ideal state (see Fig. 1b)) and thus some fiction is involved in the measurements. The particles were characterized by using laser analysis, which works with volume equivalent diameter. This implies that when the characteristic dimension of a particle is 58,9 μm it does not necessarily follow that it will pass through a sieve with a 63 μm aperture, and on the other hand, a 66,9 μm diameter does not necessarily mean that it will not pass through a sieve with a 63 μm aperture size. Furthermore, for such small particles, the electrostatic and Van der Waals forces acting between the particles also play an important role. These forces may be so strong that they do not break down due to vibrations, and therefore a particle that should fall through will not fall through the aperture.

ACKNOWLEDGEMENTS

The authors wish to acknowledge the Ministry of Education, Science, Research and Sport of the Slovak Republic for the financial support of this research by grants KEGA 036STU-4/2020 and VEGA 1/0070/22.

LIST OF SYMBOLS

r_A	recovery of coarse product	(1)
r_B	recovery of fine product	(1)
A	mass of the oversized product	(kg)
B	mass of the undersized product	(kg)
D_a	aperture size – cut size	(mm)
F	mass of the raw material	(kg)
R_A	cumulative oversize fraction of the oversized product – at D_a	(1)
R_B	cumulative oversize fraction of the undersized product – at D_a	(1)
R_F	cumulative oversize fraction of the raw material – at D_a	(1)
η	total classification efficiency	(%)

REFERENCES

[1] Keshun, L. 2009, "Some factors affecting sieving performance and efficiency", Powder Technology 193 (2), pp. 208-213, **2009**.

[2] Dong, K. J., Yu, A. B., Brake, I. DEM simulation of particle flow on a multi-deck banana screen", Minerals Engineering 22 (11), pp. 910 – 920, **2009**.

[3] Lawinska, K., Wodzinski, P., Modrzewski, R. 2014. "Verification of the mathematical model of the screen blocking process", Powder Technology 256 (4), pp. 506 – 511, **2014**.

[4] CHEN, Z. – TONG, X. – LI, Z. 2020. Numerical investigation on the sieving performance of elliptical vibrating screen", Processes 8, p. 1151, **2020**.

[5] Davoodi, A. et al. "Effects of screen decks' aperture shapes and materials on screening efficiency, Minerals Engineering 139, **2019**.

[6] Jafari, A. – Nezhad, V. S. "Employing DEM to study the impact of different parameters on the screening efficiency and mesh wear", Powder Technology vol. 297, pp. 126 – 143, **2016**.

[7] Dong, H. "Influence of vibration mode on the screening process. In: International Journal of Mining Science and Technology" 1, p. 95-98, **2013**.

[8] WANG, W. et al. "Mechanism of overcoming plugging and optimization of parameters for rigid-flexible coupled elastic screening of moist fine coal", Powder Technology 376, pp. 113 – 125, **2020**.

[9] Makinde, O. A. et al. "Review of vibrating screen development trends: Linking the past and the future in mining machinery industries", International Journal of Mineral Processing 145, pp. 17 – 22, **2015**.

[10] Jiang, H. et al. "Dynamic characteristics of an equal-thickness screen with a variable amplitude and screening analysis", Powder Technology 311, pp. 239 – 246, **2017**.

[11] Elskamp, F. "Benchmarking of process models for continuous screening based on discrete element simulations", Minerals Engineering 83, pp. 78 – 96, **2015**.

[12] Li, J. et al. "Discrete particle motion on sieves—a numerical study using the DEM simulation", Powder Technology 133 (1 – 3), pp. 190 – 202, **2003**.

[13] Yoshida, Y. et al. "Estimation equation for sieving rate based on the model for undersized particles passing through vibrated particle bed", Journal of chemical engineering of Japan 46 (2), pp. 116 – 126, **2013**.

[14] Wang, Z. et al. “Impact of screening coals on screen surface and multi-index optimization for coal cleaning production”, Journal of Cleaner Production 187, pp. 562 – 575, **2018**.

[15] Soldinger, M. “Influence of particle size and bed thickness on the screening process”, Minerals Engineering 13 (3), pp. 297 – 312, **2000**.

[16] Harish, H. et al. “The screening efficiency if linear vibrating screen – An experimental investigation”, AIP Conference Proceedings 2204 – 040002, **2020**.

[17] Macho, O., Čierny, M., Gabrišová, Ľ., Juriga, M., Ružinský, R., Peciar, P. “Dynamic Image Analysis to Determine Granule Size and Shape, for Selected High Shear Granulation Process Parameters”, Strojnícky časopis – Journal of Mechanical Engineering 69 (4), pp. 57 – 64, **2019**. DOI: 10.2478/scjme-2019-0043

[18] Peciar, P., Juriga, M., Guštafík, A., Kohútová, M., Jezsó, K. “Procesné strojníctvo – Príklady”, Bratislava: Spektrum STU, **2021**. p.127, ISBN 978-80-227-5081-3 (In Slovak)

[19] Chen, Y., Tong, “Modelling screening efficiency with vibrational parameters based on DEM 3D simulation”, Mining Science and Technology (China) 20 (4), pp. 615 – 620, **2010**.

[20] Elskamp, F., Kruggel–Emden, H. ”Review and benchmarking of process models for batch screening based on discrete element simulations”, Advanced Powder Technology 26 (3), pp. 679 – 697, **2015**.

[21] Djokovic, J. M. et al. “Screening efficiency analysis of vibrosieves with the circular vibrations”, Civil and Environmental Engineering 13 (1), pp. 77 – 83, **2017**.

[22] Yin, Z., Zhang, H., Han, T. “Simulation of particle flow on an elliptical vibrating screen using the discrete element method”, Powder Technology 302, pp. 443 – 454, **2016**.

[23] Malahayati, N. et al.. “Textural properties of laksa noodle as affected by rice flour particle size”, International Food Research Journal 18 (4), pp. 1309 – 1312, **2011**.

[24] Tóth, Á. et al. “Effects of particle size on the quality of winter wheat flour, with a special focus on macro- and microelement concentration”, Communications in Soil Science and Plant Analysis 37, pp. 2659 – 2672, **2006**.

[25] Wills, B. A., Napier–Munn, T. ”Wills' Mineral Processing Technology”, 7th edition. Chapter 8 – Industrial screening, Butterworth-Heinemann, pp. 186 – 202, **2005**.

[26] Xiao, J., Tong, X. “Particle stratification and penetration of a linear vibrating screen by the discrete element method”, International Journal of Mining Science and Technology 22 (3), pp. 357 – 362, **2012**.

[27] Zhang, B. et al. “Intelligent prediction of sieving efficiency in vibrating screens”, Shock and Vibration 2016, **2016**. DOI: 10.1155/2016/9175417

[28] Krok, A. et al. “An experimental investigation of temperature rise during compaction of pharmaceutical powders”, International Journal of Pharmaceutics 513 (1 – 2), pp. 97 – 108, **2016**.

[29] Rojas, J. et al. “Evaluation of several microcrystalline celluloses obtained from agricultural by-products”, Journal of Advanced Pharmaceutical Technology & Research 2 (3), pp. 144 – 150, **2011**.

[30] Masuda, H. et al. “Powder Technology Handbook”, 3rd edition. Boca Raton, Florida: CRC Press. p. 878, **2006**. ISBN-10: 1-57444-782-3.

[31] Barbosa-Cánovas, G. V. et al.. “Food Powders”, 1st edition. New York: Kluwer Academic/Plenum Publishers. p. 372, **2005**. ISBN: 0-306-47806-4.

[32] Peciar, P. et al. “Analysis of pharmaceutical excipient MCC Avicel PH102 using compaction equations”, Strojnícky časopis – Journal of Mechanical Engineering 66 (1), pp. 65 – 82, **2016.** DOI: 10.1515/scjme-2016-0012

[33] Rhodes, M. “Introduction to Particle Technology”, 2nd edition. Chichester: John Wiley & Sons Ltd. p. 450, **2008**. ISBN: 978-0-470-01427-1.

[34] Nofrerias, I. et al. “Comparison between Microcrystalline Celluloses of different grades made by four manufacturers using the SeDeM diagram expert system as a pharmaceutical characterization tool”, In: Powder Technology 342, pp. 780 – 788, **2019**.